

New Soluble, Coplanar Poly(naphthalene-2,6-diyl)-Type π -Conjugated Polymer, Poly(pyrimido[5,4-*d*]pyrimidine-2,6-diyl), with Nitrogen Atoms at All of the *o*-Positions. Synthesis, Solid Structure, Optical Properties, Self-Assembling Phenomena, and Redox Behavior

Takakazu Yamamoto* and Bang-Lin Lee

Chemical Resources Laboratory, Tokyo Institute of Technology, 4259 Nagatsuta, Midori-ku, Yokohama 226-8503, Japan

Received September 17, 2001; Revised Manuscript Received January 14, 2002

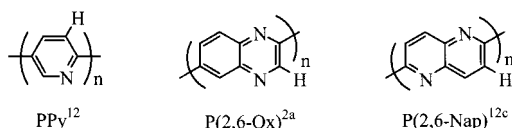
ABSTRACT: New *n*-type π -conjugated poly(pyrimido[5,4-*d*]pyrimidine-2,6-diyl)s with a poly(naphthalene-2,6-diyl)-type structure and alkylamino substituents were prepared by dehalogenative polycondensation using a zerovalent nickel complex in 90–98% yield. The polymer is considered to have a coplanar π -conjugated main chain and a strong tendency to form a π -stacked structure, as judged from its CPK molecular model, UV–vis data, photoluminescence data, and XRD data. The obtained polymers were soluble in organic solvents and a polymer with *N*-octylamino substituents showed a number-average molecular weight, M_n , of about 8000 in GPC analysis. Other polymers showed analogous M_n values. The UV–vis spectra of the polymers gave a main absorption peak at about 450 nm, which was shifted by about 130 nm to a longer wavelength compared to those of corresponding monomeric compounds. The degree of the red shift was larger than those observed with other analogous poly(naphthalene-2,6-diyl)-type π -conjugated polymers, and the large red shift was attributed to the coplanar structure of the polymer. UV–vis and photoluminescence data revealed a strong tendency for the polymer to form a self-assembled structure. Powder X-ray diffraction analysis indicated that the polymers took an end-to-end packing mode. Electrochemical reduction (or *n*-doping) of the polymers proceeded with an E_{pc} of about -2.3 V vs Ag^+/Ag .

Introduction

π -Conjugated polymers are the subject of recent interest.¹ Various π -conjugated poly(arylene)s with regulated bonding between monomeric units have been prepared by dehalogenative homopolymerization^{1–6} and copolymerization^{7–9} of dihalogenated aromatic compounds.

In cases of some five-membered ring heterocyclic homopolymers such as α -bonded polythiophene, the CPK molecular model indicates that formation of a coplanar structure is possible for the polymers. For HT (head-to-tail) poly(3-alkylthiophene)s, self-assembly of coplanar polymer molecules, which is assisted by the side-chain crystallinity, occurs, and such self-assembly brings about interesting chemical and physical properties.^{3,4,6,10,11}

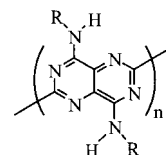
For six-membered ring π -conjugated polymers (e.g., polypyridine and poly(naphthalene-2,6-diyl)), however, the formation of a coplanar structure is usually hindered by *o*-hydrogen repulsion. Previously, we reported attempts to prepare coplanar six-membered ring π -conjugated polymers by replacing the *o*-CH groups of poly(*p*-phenylene) and poly(naphthalene) with nitrogen.¹² The following π -conjugated polymers were thus synthesized:



However, these polymers still possess *o*-hydrogen repulsion, and their limited solubility has prevented their chemical and physical properties from being well revealed. Attempts to prepare poly(pyrazine-2,5-diyl)^{12c} have not been successful.

We now report the preparation and chemical properties of the following π -conjugated poly(naphthalene-2,6-

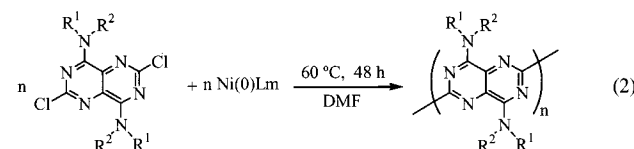
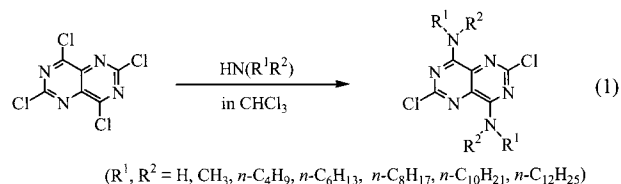
diyl)-type polymers with N atoms at all of the four *o*-positions:



The polymer is free from the *o*-H repulsion and advantageously soluble in organic solvents.

Results and Discussion

In this study, 2,6-dichloropyrimido[5,4-*d*]pyrimidines¹³ are used as the starting monomer for dehalogenative polycondensation expressed by eq 2. The monomer was



Monomers-1 through -6

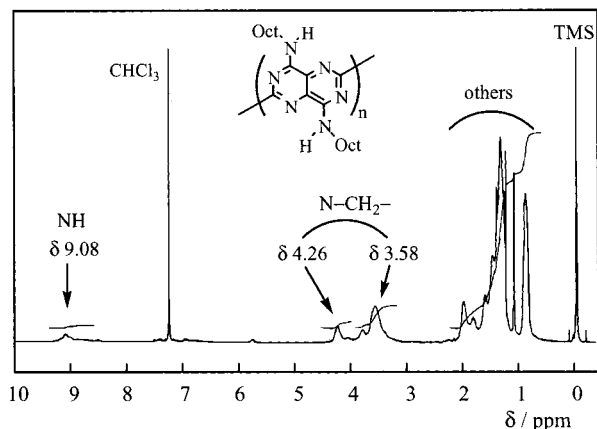
Ni(0)Lm = zerovalent nickel complex (a mixture of bis(1,5-cyclooctadiene) nickel (Ni(cod)₂) and 2,2-bipyridyl (bpy))

| R ¹ | R ² | Polymer |
|---|-----------------|-----------|
| <i>n</i> -C ₄ H ₉ | H | PPympym-1 |
| <i>n</i> -C ₈ H ₁₇ | H | PPympym-2 |
| <i>n</i> -C ₁₀ H ₂₁ | H | PPympym-3 |
| <i>n</i> -C ₁₂ H ₂₅ | H | PPympym-4 |
| <i>n</i> -C ₁₆ H ₃₃ | H | PPympym-5 |
| <i>n</i> -C ₆ H ₁₃ | CH ₃ | PPympym-6 |

Table 1. Results of the Preparation of PPypymys and UV-Vis Data of the Polymers

| no. | polymer ^a | yield, % | M_n^d | absorption, λ_{\max} , nm ^e (ϵ , M ⁻¹ cm ⁻¹) | | |
|----------------|----------------------|-----------------------|---------|--|-------------------------|------------|
| | | | | | | |
| 1 | PPypym-1 | 60 | | 445 (770) | 473 (6900) ^f | |
| 2 | PPypym-2 | 90 (60 ^c) | 8000 | 425 (7300) | 451 (7600) | 483 (3000) |
| 3 ^b | PPypym-2' | 90 | 8800 | 427 (6900) | 452 (9000) | 483 (4000) |
| 4 | PPypym-3 | 93 | 10 000 | 423 (7000) | 448 (7100) | 480 (3500) |
| 5 | PPypym-4 | 99 | 5000 | 427 (7700) | 449 (8200) | 479 (3700) |
| 6 | PPypym-5 | 98 | 7000 | 424 (7700) | 448 (8300) | 478 (3300) |
| 7 | PPypym-6 | 90 (64 ^c) | 9000 | 431 (12800) | 457 (12300) | |

^a Prepared by dehalogenation polycondensation using the nickel complex. Solvent used for polymerization = DMF, unless otherwise noted. ^b Prepared in toluene. ^c Yield after purification by reprecipitation. ^d Determined by GPC (polystyrene standards). PPypym-1; not measured due to poor solubility in chloroform. ^e Solvent = CHCl₃, unless otherwise noted. Molarity for the calculation of ϵ is based on the repeating unit. The ϵ value for the peak at the longest wavelength (478–483 nm for PPypym-2 through -5) depends on the measuring conditions. ^f Solvent = formic acid.

**Figure 1.** ¹H NMR spectrum of PPypym-2 in CDCl₃.

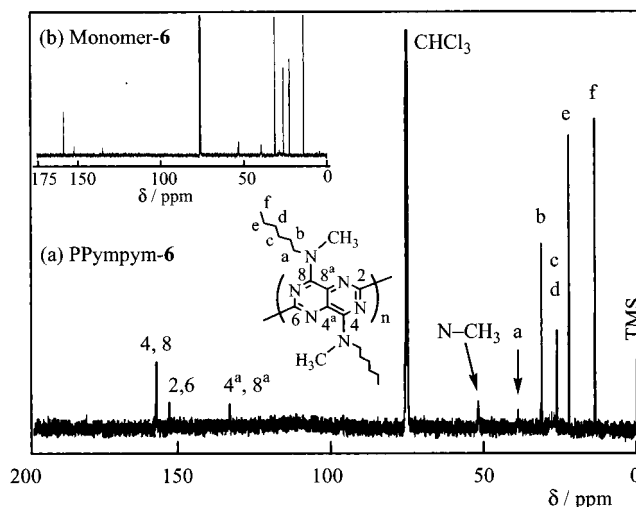
prepared by the reaction of the corresponding amine with 2,4,6,8-tetrachloropyrimido[5,4-*d*]pyrimidine as shown in eq 1.¹³ The amination took place selectively at 4 and 8 positions of the Pypym unit under mild conditions because of much lower electron density of the 4-,8-carbons than the 2-,6-carbons.

Polymerization. The above poly(pyrimido[5,4-*d*]pyrimidine-2,6-diyl)s, PPypym-1–PPypym-6, were prepared from the corresponding dihalo monomers obtained as described above using a zerovalent nickel complex (eq 2),^{2,5,6,12} and the results of the polymerization are summarized in Table 1. The polymerization proceeded well under conditions applied for analogous dehalogenative polycondensations of dihaloaromatic compounds.^{2,5}

The obtained polymers were soluble in organic solvents such as chloroform and dichloromethane, except for PPypym-1 with short butylaminogroups. PPypym-1 was soluble only in acidic solvents such as formic acid. Polymer-2 showed M_n and M_w of 8000 and 15000 (polystyrene standards), respectively, in GPC analysis. Use of toluene^{12d} as the polymerization solvent gave PPypym-2 with a comparable M_n of 8800 (cf. no. 3 in Table 1), and the polymer showed an $[\eta]$ value of 0.22 dL g⁻¹ in CHCl₃ at 30 °C.

Other polymers gave similar M_n s in GPC analysis. The polymers did not contain Cl (cf. Experimental section), similar to poly(pyridine-2,5-diyl) obtained by analogous dehalogenative polycondensation,^{12a} indicating that the polymer is terminated by a ~C–Ni bond that is converted into a ~C–H bond during workup of the polymer.

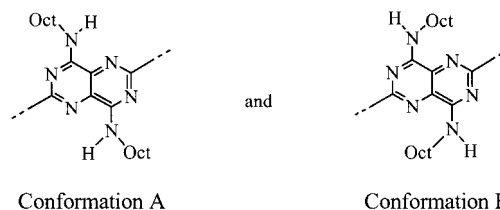
NMR and IR. Figure 1 depicts the ¹H NMR spectrum of PPypym-2 in CDCl₃. The ¹H NMR spectrum shows N–H and aliphatic-H peaks at δ 9.08 (2H) and 0.90–

**Figure 2.** ¹³C{¹H} NMR spectra of (a) PPypym-6 and (b) monomer-6 in CDCl₃.

4.26 (34H), respectively, in accord with the structure of the polymer. The N–CH₂ peak of the octyl group splits into two broad peaks at δ 4.26 and 3.58, suggesting the presence of isomeric conformations concerning the –NHOct group.

In the case of the corresponding monomer, the N–CH₂ protons give only one peak at room temperature, presumably due to the rapid rotation of the –NHOct group around the C–NHOct bond.

Conformation A seems more stable due to a steric reason: an N–H···N interaction may enhance the stability of conformation A. In the ¹³C NMR spectrum



of PPypym-2 (cf. Experimental section), the α-CH₂ and β-CH₂ peaks of the octyl group also split into two peaks, supporting the presence of isomeric structures. As exhibited in Figure 2, however, the ¹³C NMR spectrum of PPypym-6 in CDCl₃ shows simple sharp signals and the signal pattern corresponds well with that of monomer-6 (Figure 2b), suggesting that the –N(CH₃)(*n*-C₆H₁₃) group can easily rotate around the C–N(CH₃)(*n*-C₆H₁₃) bond on the NMR time scale due to the absence of the N–H···N interaction. The ¹H NMR spectrum of PPypym-6 also shows a simple peak pattern.

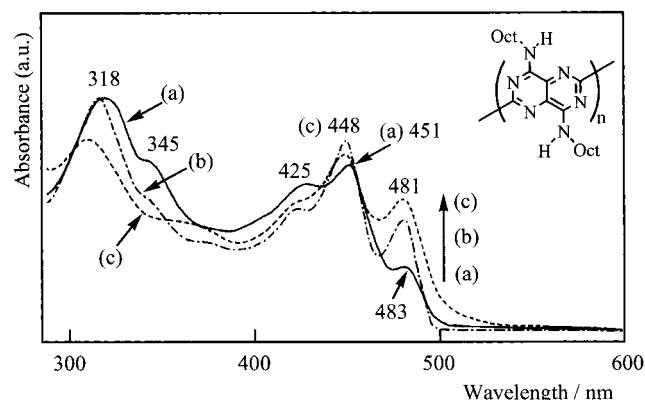


Figure 3. UV-vis spectra of PPympym-2: (a) in CHCl_3 at lower concentration ($6.5 \times 10^{-5} \text{ M}$), measured with a 1.0 cm cell (—); (b) in CHCl_3 at higher concentration ($9.1 \times 10^{-4} \text{ M}$), measured with a 0.08 cm cell (---); (c) in film cast on a quartz plate (- - -). The peak at 481 nm also rises after passing through a capillary.

IR spectra of polymers show peak patterns similar to those of the starting monomers; however, the $\nu(\text{C}-\text{Cl})$ peak of the monomer near 890 cm^{-1} completely disappeared.

UV-Vis Data. Figure 3 exhibits the UV-vis spectrum of PPympym-2. The two peaks at 318 and 345 nm are characteristic of aromatic compounds having a naphthalene-like frame,¹⁴ and assigned to $\pi-\pi^*$ transition in the monomeric unit. The main peak at 451 nm is considered to be due to $\pi-\pi^*$ transition along the polymer main chain. The subpeak at 425 nm may be due to a vibronic coupling of the electronic transition; the energy difference (approximately 1350 cm^{-1}) between the peaks at 451 and 425 nm corresponds to a ring vibration frequency of the naphthalene ring.

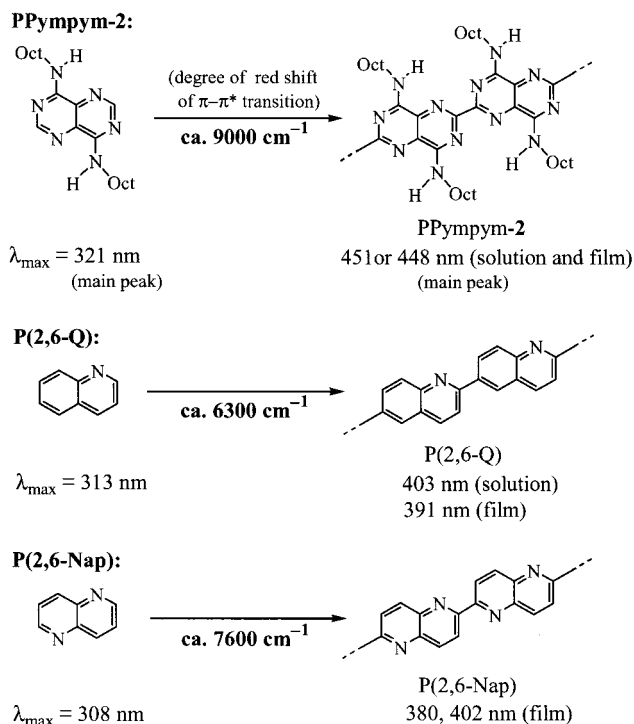
On the other hand, another subpeak at 483 nm seems to originate from self-assembled (or π -stacked) polymer molecules, since intensity of this peak increases at a higher concentration (curve b) in Figure 3, observed with a cuvette with a short optical path) and in film (curve c). It has been reported that regioregular poly(3-alkylthiophene),^{3,4,10b,11} poly(3-alkylfurane),^{6a} poly(dialkylbithiazole)s,^{6b,10b} and poly(2,5-dialkyl-*p*-phenyleneethynylene)s^{10c} also give a subpeak at a longer wavelength when they form a self-assembled π -stacked structure. The degree of the shift to a longer wavelength, 32 nm or 1500 cm^{-1} , is comparable to that observed with poly(3-alkylfurane) (1700 cm^{-1})^{6a} and smaller than those observed with poly(3-alkylthiophene)s and poly(dialkylthiazole)s (about 5000 cm^{-1} for both).^{10b} Thus, the data shown in Figure 3 indicate that such π -stacking can also occur for poly(naphthalene-2,5-diyl)-type π -conjugated polymers.

The intensity of the peak at 483 nm increased after the chloroform solution of PPympym-2 was passed through a glass capillary or a syringe filter, suggesting that the self-assembly is enhanced by molecular ordering of the polymer in a fluid solution. Such molecular ordering is well-known for aromatic polyamides (e.g., Kevlar) in fluid acidic solutions.

Other PPympyms, except for PPympym-6, give similar UV-vis data, which are summarized in Table 1.

PPympym-6 gives a main UV-vis peak near those of other PPympyms. However, it does not give the UV-vis peak assigned to the self-assembled polymer molecules, suggesting that the bulky $-\text{N}(\text{CH}_3)(n\text{-C}_6\text{H}_{13})$

Chart 1. Comparison of UV-Vis Data of Poly(naphthalene-2,6-diyl)-Type Polymers



groups in PPympym-6 interfere with the face-to-face stacking.

Comparison with Other Poly(naphthalene-2,6-diyl)-Type Polymers. Chart 1 shows a comparison of the UV-vis data of PPympym-2 with those of other poly(naphthalene-2,6-diyl)-type π -conjugated polymers.

As shown in Chart 1, the above-described main peak of PPympym-2 appears at a longer wavelength than those of poly(quinoline-2,6-diyl) P(2,6-Q)^{12b,c} ($\lambda_{\text{max}} = 403 \text{ nm}$ in formic acid and 391 nm in the solvent-free film) and poly(1,5-naphthyridine-2,6-diyl) P(2,6-Nap)^{12c} ($\lambda_{\text{max}} = 380$ and 402 nm in the solvent-free film). P(2,6-Q) and P(2,6-Nap) were not soluble in nonacidic solvents where the effect of possible protonation could be avoided. The XRD patterns of these polymers show no sign of the above-described self-assembly, and the UV-vis data of the polymer films are considered to reflect the electronic state of a *single* polymer molecule.

In Chart 1, the single arrow stands for the degree of the energy shift in the $\pi-\pi^*$ transition from the naphthalene-like monomeric unit. The data reveal that PPympym-2 exhibits a larger shift (ca. 9000 cm^{-1}) compared with those for P(2,6-Q) and P(2,6-Nap), suggesting the formation of a more effective π -conjugated system in PPympym-2. The CPK molecular model of the polymer shows that the coplanar structure of PPympym-2 receives no steric repulsion due to the absence of *o*-hydrogen. P(2,6-Q) did not give any sign of molecular assembly, presumably due to its noncoplanar structure.

Photoluminescence Data. Figure 4 shows the photoluminescence (PL) and excitation spectra of PPympym-2 in CHCl_3 and in film.

In Solution. PPympym-2 exhibits four PL peaks at 469 (main), 501, 540, and 590 nm when irradiated with 451 nm light in chloroform (Figure 4a). The position of the main PL peak, 469 nm, agrees with the onset position of the main absorption peak at 451 nm (cf. Figure 3), as is usually observed with aromatic compounds and aromatic polymers. However, the three

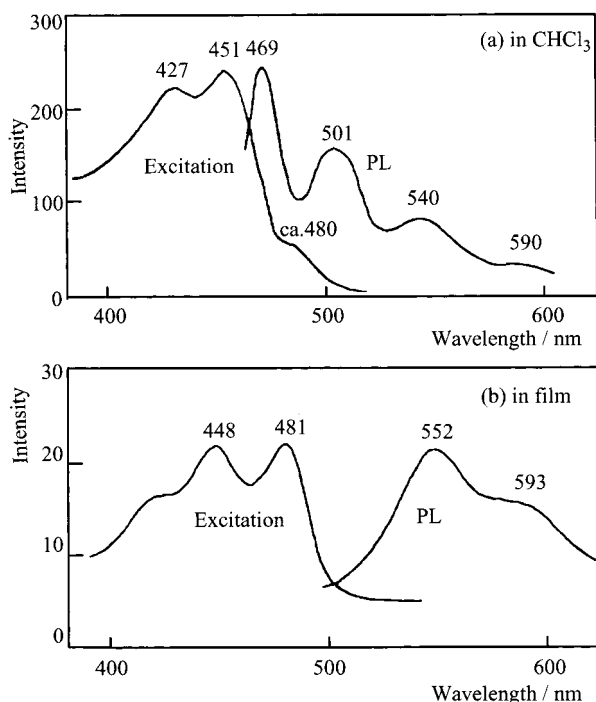


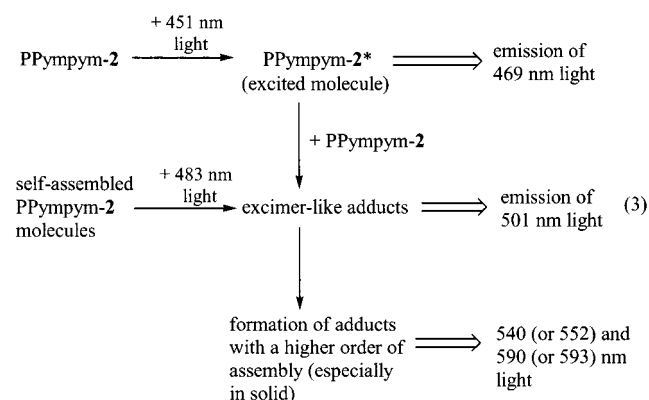
Figure 4. Photoluminescence (right) and excitation spectra (left) of PPypm-2 in (a) CHCl_3 and (b) film.

additional photoluminescence peaks in the longer wavelength are considered to originate from excimer-like adducts^{10,12} formed between photoexcited PPypm-2 and the polymer in the ground state.

The PL peak at 501 nm locates near the onset position of the UV-vis peak at 483 nm which is assigned to the self-assembled polymer molecules. The appearance of two additional PL peaks suggests the formation of adducts with a higher order of assembly in the PL process.

The excitation spectrum monitored at any of the four photoluminescence peaks shows peaks at 451 and 427 nm, agreeing with the UV-vis data of PPypm-2. The excitation spectrum monitored at 501, 540, and 590 nm exhibits a shoulder peak at about 480 nm.

In Film. For the film samples, the two peaks at 552 and 593 nm become strong, and the excitation spectrum clearly indicates a peak at 481 nm. On the basis of these results, the PL processes can be illustrated as follows:



Other polymers, except for PPypm-6, give analogous PL data which are summarized in Table 2. PPypm-6 also gives two PL peaks at 501 and 540 nm besides the normal PL peak at 476 nm (cf. Table 2),

Table 2. PL Data of the Polymers

| no. | polymer | photoluminescence, λ_{em} , nm (λ_{ex} , nm) ^a | | | | | |
|-----|---------|--|-----|-----|--------------------|-----|----------------|
| | | in solution | | | film | | |
| 1 | PPypm-1 | 491 | 527 | 566 | (445) ^c | | |
| | | 491 | 527 | 566 | (476) ^c | | |
| 2 | PPypm-2 | 469 | 501 | 540 | 552 | 593 | (448, 481) |
| | | | | 552 | 593 | | (483) |
| 3 | PPypm-3 | 467 | 498 | 550 | 592 | 551 | 581 (448, 482) |
| | | | | 550 | 592 | | (482) |
| 4 | PPypm-4 | 467 | 496 | 546 | 592 | 548 | 592 (449, 479) |
| | | | | 548 | 593 | | (479) |
| 5 | PPypm-5 | 464 | 495 | 544 | 591 | 549 | 590 (448, 478) |
| | | | | 548 | 592 | | (478) |
| 6 | PPypm-6 | 476 | 508 | 547 | (457) | 555 | (457) |

^a The wavelength of excitation light (λ_{ex}) is given in parentheses.
^b Solvent = CHCl_3 , unless otherwise noted. ^c Measured in formic acid.

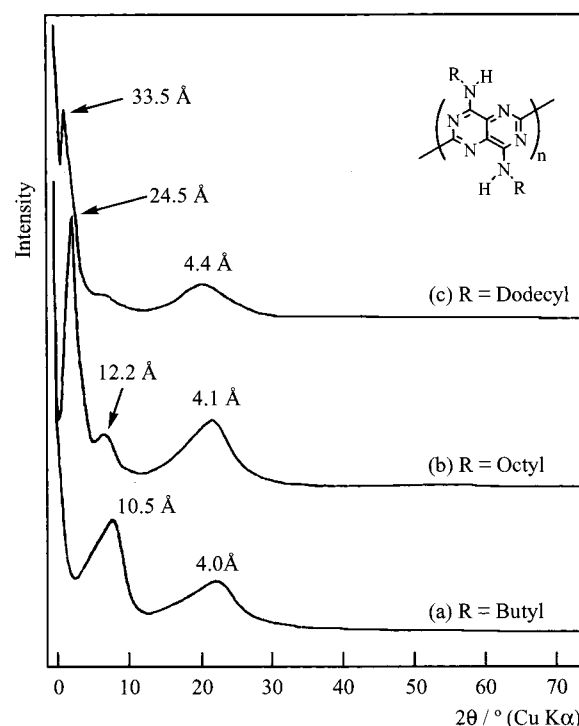


Figure 5. Powder X-ray diffraction patterns of (a) PPypm-1, (b) PPypm-2, and (c) PPypm-4.

indicating that formation of the excimer-like adduct is also possible with the polymer. However, PPypm-6 shows no PL peak at about 590 nm in CHCl_3 and in film.

XRD Data and Packing Structure. Figure 5 exhibits powder X-ray diffraction (XRD) patterns for PPypm-1, -2, and -4. All of the XRD patterns show a diffraction peak in the low-angle region. This peak is characteristic of π -conjugated aromatic polymers that have long side chains and take a stacked structure in the solid assisted by side chain crystallinity. Regioregular poly(3-alkylthiophene),^{3,4,10a} poly(3-alkyl-furane),^{6a} poly(dialkylthiazole)s,^{10a} poly(dialkoxanthraquinone),¹⁵ and poly(dialkoxyp-phenylene)¹⁶ show an XRD peak in the same region, and the d value of the peak is assigned to the distance between the π -conjugated main chains separated by the alkyl groups. The distances of 10.55, 24.5, and 33.5 Å observed for PPypm-1, -2, and -4, respectively, are also most probably assignable to the distance between the polymer main chains separated by the alkyl groups. The peak of PPypm-2 at $d = 12.2$ Å is assigned to the second-order peak ($d = 24.5$

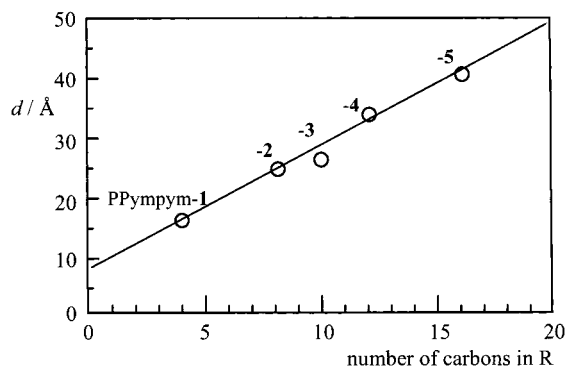


Figure 6. Plots of the d value vs the number of carbons in the R group in the polymer.

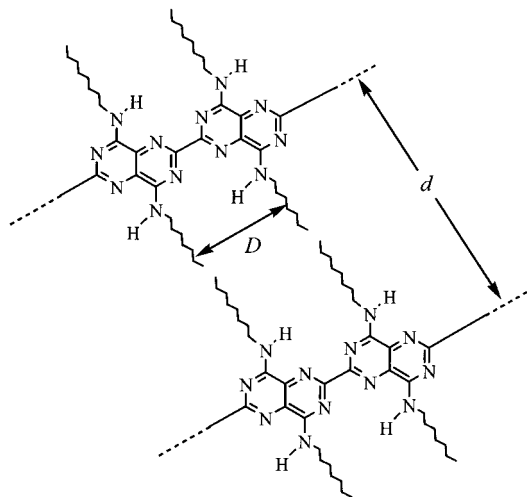


Figure 7. End-to-end packing model for PPypm-2. The polymer molecules are considered to form a sheet. In the sheet below the upper layer, the pyrimidopyrimidine ring of the polymer is supposed to occupy an intermediate position between the two pyrimidopyrimidine rings in the upper layer; thus, an effective accumulation of the side chain is attained.

$\text{\AA}/n$; $n = 2$) of the diffraction at $d = 24.5 \text{ \AA}$.

The broad peak at about $d = 4.1 \text{ \AA}$ corresponds to the distance between packed alkyl chains;¹⁷ however, the peak may contain contribution from the face-to-face packing of the polymer plane. The face-to-face packing distance will be in a range of $3.7\text{--}4.0 \text{ \AA}$, as observed with other π -conjugated polymers taking the face-to-face packed structure.^{3,4,6a,10a,16}

As shown in Figure 6, plots of the d value, which is calculated from the peak in the low-angle region, vs the number of carbons in the alkyl (R^1) chain give a straight line. These data support the above-described assumption.

Figure 7 depicts an end-to-end packing model for PPypm-2. The CPK molecular model gives a D value of 6.6 \AA in Figure 7. In view of the effective diameter (5.0 \AA)^{10a,15,17} of the R group, the polymer is considered to assume an end-to-end packing mode rather than an interdigitation packing mode. The slope of the line in Figure 6, $2.13 \text{ \AA}/\text{carbon}$, agrees with the end-to-end packing mode since one CH_2 unit has a height of 1.25 \AA .¹⁷ The intercept of the straight line in Figure 6, about 8 \AA , also agrees with the effective thickness of the polymer main chain.

Electrochemical Properties. Figure 8 shows the cyclic voltammogram (CV) of a cast film of PPypm-2 on a Pt plate in an acetonitrile solution of $[(\text{C}_2\text{H}_5)_4\text{N}]\text{BF}_4$

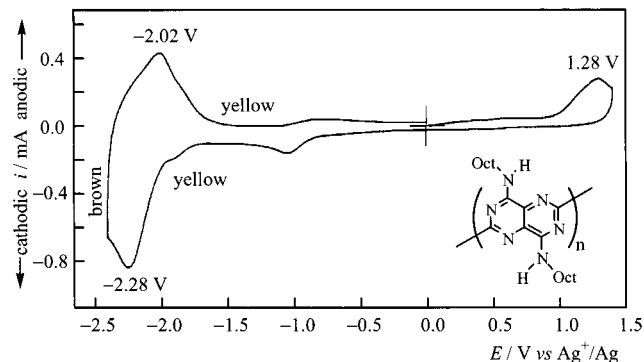


Figure 8. Cyclic voltammogram of a film of PPypm-2 on a Pt plate in an acetonitrile solution of $[(\text{C}_2\text{H}_5)_4\text{N}]\text{BF}_4$ (0.10 M). Sweep rate is 70 mV s^{-1} at room temperature.

Table 3. Redox Potentials and Doping Levels of the Polymers

| no. | polymer ^a | redox potential, V vs Ag^+/Ag ^b | | | doping level ^c |
|-----|----------------------|--|---------------------------------|-------|---------------------------|
| | | n -doping (E_{pc}) | p -doping (E_{pa}) | E^b | |
| 1 | PPypm-2 | -2.28 | -2.02 | -2.15 | 0.49 |
| 2 | PPypm-3 | -2.30 | -2.06 | -2.18 | 0.23 |
| 3 | PPypm-4 | -2.44 | -2.08 | -2.26 | 0.15 |
| 4 | PPypm-6 | -2.36 | -2.15 | -2.26 | 0.49 |

^a PPypm-1: Not measured due to difficulty of preparing a good cast film. PPypm-5: No peak was observed up to -2.7 V vs Ag^+/Ag . ^b Measured in an acetonitrile solution of $[(\text{C}_2\text{H}_5)_4\text{N}]\text{BF}_4$ (0.1 M). E_{pa} = peak anodic potential, E_{pc} = peak cathodic potential, and E^b = the average of E_{pa} and E_{pc} . ^c The number of negative charges stored per repeating unit.

BF_4 (0.10 M). Electrochemical reduction (n -doping) starts at about -2 V vs Ag^+/Ag with a peak at $E_{\text{pc}} = -2.28 \text{ V}$ vs Ag^+/Ag . Reverse scanning gives an oxidation (n -undoping) peak at $E_{\text{pa}} = -2.02 \text{ V}$ vs Ag^+/Ag . The electrochemical processes are accompanied by color changes, as exhibited in Figure 8.

The electrochemical reduction requires a negative potential comparable to or somewhat larger than those of P(2,6-Q) ($E_{\text{pc}} = -2.25 \text{ V}$ vs Ag^+/Ag)^{12b} and P(2,6-Nap) ($E_{\text{pc}} = -1.9 \text{ V}$ vs Ag^+/Ag),^{12c} despite the presence of a larger number of electron-withdrawing imine nitrogens in PPypm-2. This is attributed to the electron-donating NHR groups attached to the pyrimidopyrimidine ring.

Table 3 summarizes the redox data of the present polymers. As shown in nos. 1–3 in Table 3, an increase in the length of the alkyl substituent causes a shift of the n -doping (E_{pc}) potential from -2.28 V vs Ag^+/Ag (the value for PPypm-2) to a negatively higher potential. CV of PPypm-5 with a very long cetyl ($n\text{-C}_{16}\text{H}_{33}$) group shows no reduction (n -doping) peak up to -2.7 V vs Ag^+/Ag . The increase in the electron-donating ability of the alkyl group with its length and the insulating effect of the alkyl group account for the shift in the reduction potential. As shown in Figure 8, the polymer also showed a smaller oxidation peak at 1.28 V vs Ag^+/Ag . However, its corresponding reduction peak was not clearly observable, presumably due to a strong interaction between the oxidized polymer species and the anion (BF_4^-).

Electrochromism. Figure 9 exhibits changes of the UV–vis absorption spectrum of a cast film of PPypm-2 on an ITO (indium–tin–oxide) glass electrode upon application of reduction potentials of -2.0 to -2.7 V vs Ag^+/Ag . At -2.2 V vs Ag^+/Ag , where the polymer is

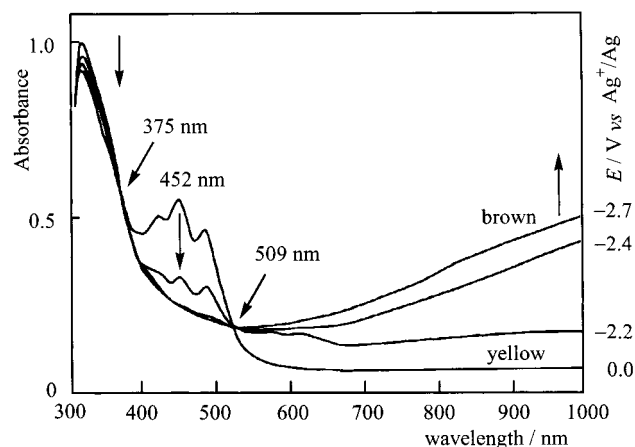


Figure 9. Changes in the UV-vis absorption spectrum of a film of PPypym-2 on an ITO electrode during electrochemical reduction (n-doping) in an acetonitrile solution of $[(C_2H_5)_4N]BF_4$ (0.10 M).

moderately reduced, the π - π^* absorption band of the polymer main chain at 452 and 483 nm decreases and a new absorption band appears at a longer wavelength above 1000 nm. Determination of the peak position was not feasible due to the absorption by the ITO glass in the longer wavelength region. Upon application of negatively high potentials of -2.4 and -2.5 V vs Ag^+/Ag , the original π - π^* absorption band disappeared completely, and only the new broad absorption band in the infrared region was observed. Various n-type conducting poly(arylene)s have been reported to show similar spectroscopic changes on electrochemical reduction (electrochromism).^{2a,12,18}

Conclusions

New soluble, coplanar π -conjugated polymers of pyrimido[5,4-*d*]pyrimidine with alkylamino groups have been prepared by organometallic polycondensation in high yields. The obtained polymers are soluble in organic solvents. The polymers show UV-vis absorption peaks at about 450 nm; the peak position locates at the longest wavelength among those of π -conjugated poly(naphthalene-2,6-diyl)-type polymers. The UV-vis and PL data of the polymers reveal an inclination of the polymer to form a self-assembled structure both in $CHCl_3$ and in film. Powder XRD data support the view that the polymers take an end-to-end packing mode. The electrochemical n-doping of the cast films of the polymers is accompanied by changes in the UV-vis spectrum (electrochromism).

Experimental Section

Materials and Measurements. Phosphoryl chloride and phosphorus pentachloride PCl_5 were purchased from Wakco Pure Chemical Industries, Ltd. *N*-Alkylamine (alkyl: butyl, octyl, decyl, dodecyl, cetyl), *N,N*-methylhexylamine, 2,2-bipyridyl (bpy), and 1,5-cyclooctadiene (cod) were purchased from Kanto Chemical Co., Inc. Bis(1,5-cyclooctadiene) nickel(0), $Ni(cod)_2$, was prepared according to the literature.¹⁹ *N,N*-Dimethylformamide (DMF) was dried, distilled under N_2 , and stored under N_2 . 2,4,6,8-Tetrachloropyrimido[5,4-*d*]pyrimidine was synthesized according to the literature.¹³ The analytical data agreed. Anal. Calcd for $C_6N_4Cl_4$: C, 26.7; N, 20.8; Cl, 52.5. Found: C, 26.7; N, 20.4; Cl, 52.5. IR (KBr, cm^{-1}): 1583, 1523, 1429, 1392, 1294, 1196, 1128, 889, 805, 615. $^{13}C\{^1H\}$ NMR ($CDCl_3$, ppm): δ 165.62 (4,8-C), 157.60 (2,6-C), 141.76 (4^a, 8^a-C).

NMR (1H and ^{13}C) and IR spectra were recorded on a JEOL EX-400 spectrometer and a JASCO IR-800 spectrometer, respectively. GPC curves were obtained with a Shimadzu liquid chromatography system with a Shodex 80 M column and a 6A refractive index detector: eluent = $CHCl_3$. UV-vis and photoluminescence spectra were reported on a Shimadzu UV-3100 and a Hitachi F-4010 spectrometer, respectively. Cyclic voltammetry was performed with a Hokuto Denko HA-501 galvanostat/potentiostat and a Hokuto Denko KB-104 function generator.

2,6-Dichloro-4,8-bis(*N*-octylamino)pyrimido[5,4-*d*]pyrimidine (Monomer-2). A chloroform solution (40 mL) of 2,4,6,8-tetrachloropyrimido[5,4-*d*]pyrimidine (0.32 g, 1.2 mmol) was cooled to -10 °C, and a chloroform solution (10 mL) of octylamine (0.78 g, 6.0 mmol) was added dropwise with stirring. The reaction mixture was stirred for 30 min below 10 °C, followed by removal of chloroform under reduced pressure at room temperature to afford a white solid. The white solid was purified by column chromatography on a silica gel column using $CHCl_3$ as an eluent to afford a white solid (0.47 g, yield = 87%). Mp = 91 – 92 °C. Anal. Calcd for $C_{12}H_{36}N_6Cl_2$: C, 58.0; H, 8.0; N, 18.5; Cl, 15.6. Found: C, 57.6; H, 7.6; N, 18.2; Cl, 15.7. IR (KBr, cm^{-1}): 3286, 2960, 2926, 2850, 1586, 1527, 1471, 1435, 1350, 974, 886, 742. 1H NMR ($CDCl_3$, ppm): δ 6.86 (t, 2H, J = 5.37 Hz, NH), 3.57 (q, 4H, J = 6.25 Hz, N- CH_2), 1.68 (m, 4H, CH_2), 1.36 (m, 20H, $(CH_2)_5$), 0.88 (t, 6H, CH_3). $^{13}C\{^1H\}$ NMR ($CDCl_3$, ppm): δ 159.28 (4,8-C), 156.50 (2,6-C), 131.63 (4^a, 8^a-C), 41.17 (C¹ of octyl group), 31.76 (C²), 29.18 (C³), 29.14 (C⁴), 28.99 (C⁵), 26.84 (C⁶), 22.61 (C⁷), 14.05 (C⁸).

Preparation of other pyrimido[5,4-*d*]pyrimidine monomers (monomer-1 to -6) was carried out analogously, and the obtained monomers gave satisfactory analytical data.

2,6-Dichloro-4,8-bis(*N*-butylamino)pyrimido[5,4-*d*]pyrimidine (Monomer-1). White solid. Yield = 56%. Mp = 102 – 104 °C. Anal. Calcd for $C_{14}H_{20}N_6Cl_2$: C, 49.0; H, 5.9; N, 24.5; Cl, 20.7. Found: C, 48.8; H, 5.7; N, 24.3; Cl, 20.6. IR (KBr, cm^{-1}): 3284, 2930, 2868, 1588, 1528, 1432, 1351, 882, 742. 1H NMR ($CDCl_3$, ppm): δ 6.86 (t, 2H, NH), 3.58 (q, 4H, N- CH_2), 1.68 (m, 4H, CH_2), 1.44 (m, 20H, CH_2), 0.97 (t, 6H, CH_3). $^{13}C\{^1H\}$ NMR ($CDCl_3$, ppm): δ 159.40 (4,8-C), 156.58 (2,6-C), 131.73 (4^a, 8^a-C), 40.98 (C¹ of the butyl group), 31.14 (C²), 20.13 (C³), 13.82 (C⁴).

2,6-Dichloro-4,8-bis(*N*-dodecylamino)pyrimido[5,4-*d*]pyrimidine (Monomer-4). White solid. Yield = 86%. Mp = 100 – 102 °C. Anal. Calcd for $C_{30}H_{52}N_6Cl_2$: C, 63.5; H, 9.2; N, 14.8; Cl, 12.5. Found: C, 63.1; H, 9.2; N, 14.9; Cl, 12.6. IR (KBr, cm^{-1}): 3274, 2916, 2850, 1591, 1531, 1470, 1435, 1349, 890, 742. 1H NMR ($CDCl_3$, ppm): δ 6.86 (t, 2H, NH), 3.57 (q, 4H, N- CH_2), 1.68 (m, 4H, CH_2), 1.35 (m, 36H, $(CH_2)_9$), 0.88 (t, 6H, CH_3). $^{13}C\{^1H\}$ NMR ($CDCl_3$, ppm): δ 159.28 (4,8-C), 156.50 (2,6-C), 131.63 (4^a, 8^a-C), 41.17 (C¹ of the dodecyl group), 31.90 (C²), 29.60 (C³⁻⁵), 29.47, 29.32, 29.23, 28.99, 26.82, 22.67, and 14.11 (C⁶–C¹²).

2,6-Dichloro-4,8-bis(*N*-methylhexylamino)pyrimido[5,4-*d*]pyrimidine (Monomer-6). White solid. Yield = 76%. Mp = 91 – 92 °C. Anal. Calcd for $C_{20}H_{32}N_6Cl_2$: C, 56.2; H, 7.5; N, 19.7; Cl, 16.6. Found: C, 56.5; H, 6.9; N, 19.8; Cl, 16.7. IR (KBr, cm^{-1}): 2954, 2924, 2856, 1548, 1536, 1503, 1414, 1395, 1147, 1047, 903, 735. 1H NMR ($CDCl_3$, ppm): δ 4.15 (broad, 6H, N- CH_3), 3.28 (b, 4H, N- CH_2), 1.72 (b, 4H, CH_2), 1.34 (b, 12H, $(CH_2)_3$), 0.90 (t, 6H, CH_3). $^{13}C\{^1H\}$ NMR ($CDCl_3$, ppm): δ 159.26 (4,8-C), 153.02 (2,6-C), 135.94 (4^a, 8^a-C), 53.52 (N- CH_3), 39.84 (C¹ of hexyl group), 31.54 (C²), 26.34 (C^{3,4}), 22.59 (C⁵), 14.01 (C⁶).

4,8-Bis(*N*-octylamino)pyrimido[5,4-*d*]pyrimidine (the Monomeric Compound Depicted in Chart 1). This compound was obtained as a white powder from 4,8-dichloropyrimido[5,4-*d*]pyrimidine by modifying the procedure in the literature.¹³ Yield = 92%. Mp = 57 – 58 °C. Anal. Calcd for $C_{22}H_{38}N_6$: C, 68.3; H, 9.9; N, 21.7. Found: C, 68.0; H, 9.5; N, 21.6. IR (KBr, cm^{-1}): 2920, 2852, 1566, 1536, 1425, 1388, 1355, 1330, 867, 836, 636. 1H NMR ($CDCl_3$, ppm): δ 8.47 (s, 2H, 2- and 6-H of Pypym ring), 6.85 (t, 2H, J = 5.37 Hz, NH), 3.58 (q, 4H, J = 6.25 Hz, N- CH_2), 1.70 (m, 4H, CH_2), 1.36 (m, 20H,

(CH₂)₅, 0.88 (t, 6H, CH₃). ¹³C{¹H} NMR (CDCl₃, ppm): δ 158.93 (4,8-C), 154.60 (2,6-C), 131.33 (4^a, 8^a-C), 40.85 (C¹ of octyl group), 31.79 (C²), 29.27 (C³), 29.23 (C⁴), 29.18 (C⁵), 26.96 (C⁶), 22.63 (C⁷), 14.07 (C⁸).

Polymerization. The polymers were prepared by using an Ni(0) complex. Details of the preparation as well as analytical and spectroscopic data of the polymers are described below.

PPympym-2. To a DMF solution (20 mL) containing Ni(cod)₂ (0.40 g, 1.5 mmol), cod (0.3 mL), and bpy (0.26 g, 1.6 mmol) was added 2,6-dichloro-4,8-bis(*N*-octylamino)pyrimido-[5,4-*d*] pyrimidine (0.46 g, 1.0 mmol) with stirring. The reaction mixture was stirred at 60 °C for 48 h to afford a red precipitate. The precipitate was collected by filtration, washed with aqueous ammonia, a warm aqueous solution of EDTA (ethylenediaminetetraacetic acid), warm distilled water, and methanol in this order. Drying under vacuum at 60 °C for 40 h gave an orange-red powder of the polymer, PPympym-2, in 90% yield. The obtained polymer was further dissolved in CHCl₃ and reprecipitated in acetone to give samples for the instrumental analysis (yield = 60%). Anal. Calcd for (C₂₂H₃₆N₆·0.2H₂O)_n: C, 68.1; H, 9.5; N, 21.7. Found: C, 68.0; H, 9.6; N, 20.3. IR (KBr, cm⁻¹): 3290, 2924, 2854, 1591, 1465, 1387, 1141, 865, 720, 673. ¹H NMR (CDCl₃, ppm): δ 9.08 (2H, NH), 1.2–4.4 (28H, CH₂), 0.90 (6H, CH₃). ¹³C{¹H} NMR (CDCl₃, ppm): δ 159.39 (4,8-C), 157.07 (2,6-C), 131.96 (4^a, 8^a-C), 41.74 and 41.08 (C¹ of the octyl group), 32.03 and 31.87 (C²), 31.83 to 28.83 (C³, C⁴ and C⁵), 27.68 and 27.29 (C⁶), 22.78 and 22.67 (C⁷), 14.11 (C⁸). *M_n*/*M_w* (GPC: polystyrene standards in CHCl₃) = 8000/15000. $[\eta]$ = 0.15 dL g⁻¹ (in CHCl₃ at 30 °C).

Other polymers were prepared analogously.

PPympym-1. Dark red powder (yield = 60%). Anal. Calcd for (C₁₄H₂₀N₆·0.58H₂O)_n: C, 59.4; H, 7.5; N, 29.7. Found: C, 59.1; H, 7.3; N, 28.4. IR (KBr, cm⁻¹): 3302, 2958, 2930, 2870, 1584, 1524, 1413, 1379, 1142, 857, 724, 671.

PPympym-3. Yellow powder (yield = 93%). Anal. Calcd for (C₂₆H₄₄N₆·1.0H₂O)_n: C, 68.1; H, 10.1; N, 18.3. Found: C, 68.6; H, 9.8; N, 18.1. IR (KBr, cm⁻¹): 3290, 2924, 2852, 1588, 1528, 1382, 1230, 1140, 857, 719, 672. *M_n* = 10 000 (*M_w*/*M_n* = 3.16).

PPympym-4. Dark red powder (yield = 99%). Anal. Calcd for (C₃₀H₅₂N₆·2.5H₂O)_n: C, 66.5; H, 10.6; N, 15.5. Found: C, 66.3; H, 9.9; N, 15.4. IR (KBr, cm⁻¹): 3278, 2922, 2852, 1590, 1530, 145, 1388, 1141, 857, 719, 673. ¹H NMR (CDCl₃, ppm): δ 9.08 (2H, NH), 1.3–4.2 (44H, CH₂), 0.987 (6H, CH₃). *M_n* = 5000 (*M_w*/*M_n* = 1.23).

PPympym-5. Dark red powder (yield = 98%). Anal. Calcd for (C₃₈H₆₈N₆)_n: C, 74.9; H, 11.2; N, 13.8. Found: C, 73.1; H, 10.9; N, 13.3; Cl, 0.3. IR (KBr, cm⁻¹): 3290, 2918, 2850, 1594, 1538, 1467, 1388, 1140, 857, 718. *M_n* = 7000 (*M_w*/*M_n* = 1.24).

PPympym-6. Orange-red powder (yield = 90%). Anal. Calcd for (C₂₀H₃₂N₆)_n: C, 67.4; H, 9.0; N, 23.6. Found: C, 67.1; H, 9.0; N, 23.2. IR (KBr, cm⁻¹): 2954, 2926, 2854, 1529, 1493, 1412, 1369, 1138, 1090, 857, 740. ¹H NMR (CDCl₃, ppm): δ 3.28–4.82 (10H, N–CH₃ and N–CH₂), 1.72 and 1.25 (16H, CH₂), 0.79 (6H, CH₃). ¹³C{¹H} NMR (CDCl₃, ppm): δ 160.33 (4,8-C), 155.98 (2,6-C), 136.39 (4^a, 8^a-C), 52.80 (N–CH₃), 39.54 (C¹ of the hexyl group), 32.32 (C²), 31.82 (C³), 28.38 (C⁴), 26.74 (C⁵), 22.66 (C⁶). *M_n* = 9000 (*M_w*/*M_n* = 1.79).

References and Notes

- (1) (a) Skotheim, T. A.; Elsenbaumer, R. L.; Reynolds, J. P. *Handbook of Conducting Polymers*, 2nd ed.; Marcel Dekker: New York, 1997. (b) Nalwa, H. S. *Handbook of Organic Conductive Molecules and Polymers*; John Wiley: New York, 1997.
- (2) (a) Yamamoto, T.; Sugiyama, K.; Kushida, T.; Inoue, T.; Kanbara, T. *J. Am. Chem. Soc.* **1996**, *118*, 3930. (b) Yamamoto, T. *Bull. Chem. Soc. Jpn.* **1999**, *72*, 621. (c) Yamamoto, T.; Yamamoto, A. *Chem. Lett.* **1977**, 353.
- (3) (a) McCullough, R. D.; Lowe, R. D. *J. Chem. Soc., Chem. Commun.* **1992**, 70. (b) McCullough, R. D.; Tristram-Nagle, S.; Williams, S. P.; Lowe, R. D.; Jayaraman, M. *J. Am. Chem. Soc.* **1993**, *115*, 4910. (c) McCullough, R. D. *Adv. Mater.* **1998**, *10*, 93.
- (4) (a) Chen, T.-A.; Rieke, R. D. *J. Am. Chem. Soc.* **1992**, *114*, 10087. (b) Chen, T.-A.; Wu, X.; Rieke, R. D. *J. Am. Chem. Soc.* **1995**, *117*, 233.
- (5) Setayesh, S.; Grimsdale, A. C.; Weil, T.; Enkelmann, V.; Müllen, K.; Meghdadi, F.; List, E. J. W.; Leising, G. *J. Am. Chem. Soc.* **2001**, *123*, 946.
- (6) (a) Politis, J. K.; Nemes, J. C.; Curtis, M. D. *J. Am. Chem. Soc.* **2001**, *123*, 2537. (b) Nanos, J. I.; Kampf, J. W.; Curtis, M. D.; Gonzalez, L.; Martin, D. C. *Chem. Mater.* **1995**, *7*, 2332.
- (7) (a) Bunz, U. H. F. *Chem. Rev.* **2000**, *100*, 1605. (b) Sanechika, K.; Yamamoto, T.; Yamamoto, A. *Bull. Chem. Soc. Jpn.* **1984**, *57*, 752. (c) Yamamoto, T.; Yamada, W.; Takagi, M.; Kizu, K.; Maruyama, T.; Ooba, N.; Tomaru, S.; Kurihara, T.; Kaino, T.; Kubota, K. *Macromolecules* **1994**, *27*, 6620.
- (8) Peng, Z. G.; Gharavi, A. R.; Yu, L. *J. Am. Chem. Soc.* **1997**, *119*, 4622.
- (9) Hu, Q.-S.; Vitharana, D.; Liu, G.; Jain, V.; Pu, L. *Macromolecules* **1996**, *29*, 5075.
- (10) (a) Yamamoto, T.; Komarudin, D.; Arai, M.; Lee, B.-L.; Suganuma, H.; Asakawa, N.; Inoue, Y.; Kubota, K.; Sasaki, S.; Fukuda, T.; Matsuda, H. *J. Am. Chem. Soc.* **1998**, *120*, 2047. (b) Yamamoto, T.; Lee, B.-L.; Suganuma, H.; Sasaki, S. *Polym. J.* **1998**, *30*, 853. (c) Halkyard, C. E.; Rampey, M. E.; Kloppenburg, L.; Studer-Martinez, S. L.; Bunz, U. H. F. *Macromolecules* **1998**, *31*, 8655.
- (11) (a) Jérôme, D.; Bechgaard, K. *Nature (London)* **2001**, *410*, 162. (b) Schöne, J. H.; Dodabalapur, A.; Bao, Z.; Kloc, Z. B.; Schenkar, O.; Batlogg, B. *Nature (London)* **2001**, *410*, 189. (c) Sirringhaus, H.; Brown, P. J.; Friend, R. H.; Nielsen, M. M.; Bechgaard, K.; Langeveld-Boss, B. M. W.; Spiering, J. H.; Janssen, R. A. J.; Maijer, E. W.; Herwig, P.; Leeuw, D. M. *Nature (London)* **1999**, *401*, 685. (d) Yamamoto, T.; Kokubo, H.; Morikita, T. *J. Polym. Sci., Part B: Polym. Phys.* **2001**, *39*, 1713.
- (12) (a) Yamamoto, T.; Maruyama, T.; Zhou, Z.-H.; Ito, T.; Fukuda, T.; Yoneda, Y.; Begum, F.; Ikeda, T.; Sasaki, S.; Takezoe, H.; Fukuda, A.; Kubota, K. *J. Am. Chem. Soc.* **1994**, *116*, 4832. (b) Saito, N.; Kanbara, T.; Nakamura, Y.; Yamamoto, T.; Kubota, K. *Macromolecules* **1994**, *27*, 756. (c) Saito, N.; Yamamoto, T. *Macromolecules* **1995**, *28*, 4260. (d) Yamamoto, T.; Wakabayashi, S.; Osakada, K. *J. Organomet. Chem.* **1982**, *428*, 223. (e) Yamamoto, T.; Nakamura, T.; Fukumoto, H.; Kubota, K. *Chem. Lett.* **2001**, 502.
- (13) (a) Fischer, F. G.; Roch, J.; Neumann, W. P. *Justus Liebigs Ann. Chem.* **1960**, *631*, 147. (b) Fischer, F. G.; et al. US Patent 3,031,450. Patented Apr 24, 1962. (c) Yamamoto, T.; Lee, B.-L. *Tetrahedron Lett.* **1999**, *40*, 535.
- (14) Wait, S. C.; Wesley, J. W. *J. Mol. Spectrosc.* **1966**, *19*, 25.
- (15) (a) Muramatsu, Y.; Yamamoto, T. *Polymer* **1999**, *40*, 6607. (b) Muramatsu, Y.; Yamamoto, T.; Hasegawa, M.; Yagi, T.; Koinuma, H. *Polymer* **2001**, *42*, 6673.
- (16) Vahlenkamp, T.; Wegner, G. *Macromol. Chem. Phys.* **1994**, *195*, 1993.
- (17) (a) Watanabe, J.; Harkness, B. R.; Sone, M.; Ichimura, H. *Macromolecules* **1994**, *27*, 507. (b) Jordan, E. F., Jr.; Feldisen, D. W.; Wrigley, A. N. *J. Polym. Sci., Part A-1* **1971**, *9*, 1835.
- (18) (a) Yamamoto, T.; Etori, H. *Macromolecules* **1995**, *28*, 3371. (b) Lee, B.-L.; Yamamoto, T. *Macromolecules* **1999**, *32*, 1375.
- (19) Bogdanovic, B.; Kroner, M. *Justus Liebigs Ann. Chem.* **1966**, *699*, 1.

MA011632O